Isolated Thick Filaments of Limulus Striated Muscle in Suspension

Renliang Xu,[†,‡] Shih-fang Fan,[§] Tadakazu Maeda,[∥] and Benjamin Chu*[,†,⊥]

Department of Chemistry, Department of Anatomical Sciences, Health Sciences Center, and Department of Materials Science and Engineering, State University of New York at Stony Brook, Stony Brook, New York 11794, and Mitsubishi Kasei Institute of Life Sciences, Machida, Tokyo 194, Japan

Received April 11, 1990; Revised Manuscript Received July 7, 1990

ABSTRACT: Dynamic light-scattering (self-beating) measurements at a scattering angle of only ~3° in suspensions of isolated thick myofilaments with a length of 4 μm were accomplished by means of a prism-cell light-scattering spectrometer in combination with an in situ filtration system. With the ultra-small-angle time correlation function data as the base line, contributions due to rotational and bending motions of the filament could be computed from theoretical models and compared with the experimental average characteristic line width, $\bar{\Gamma}$, measured at large scattering angles.

I. Introduction

It is well established that the contraction of striated muscle is caused by the sliding of thick and thin filaments.[1,2] In vertebrate striated muscle the thick filament is essentially an aggregation of myosin molecules. In invertebrate striated muscle, it also contains paramyosin. The structure of the thick filament is basically a shaft with projections (cross bridges). Force is generated by repeated cycles of attachment, sliding, and detachment of the cross bridges with thin filaments. The study of cross-bridge motions is at the leading edge of contemporary muscle research. Techniques that allow direct detections of such motions are of obvious importance. Dynamic light scattering (DLS) is one such method that can detect translational motions of the center of mass of the scatterer and the internal motions of the scatterer. In DLS, there can be no complications caused by probe molecules since none are required. In the past, DLS has been employed successfully in studying the cross-bridge motions of isolated Limulus thick myofilaments. At scattering angles higher than 15°, cross-bridge motion activated by calcium ions had been detected.[3-5] Many reports have also shown that DLS could be used to study the dynamics of muscle fibers and their substructures including the bending of myofilaments, the translational diffusion of isolated myofibrils and the dynamics of muscle during tetanus (for examples, see refs 6-10).

In view of the micron characteristic dimension of the thick filaments, DLS has to be performed at ultra-small angles where the product of the scattering vector K ($\equiv 4\pi n \sin(\theta/2)/\lambda_0$, with n, λ_0 and θ being the refractive index of the solvent, the incident light wavelength in vacuo, and the scattering angle, respectively) and the filament length L, KL, is close to unity in order to obtain unbiased information on the overall dimension and the translational diffusion of muscle filaments in suspension. At $KL > 1$, rotational and internal motions contribute to the intensity-intensity time correlation function.

In the present study we used a specially designed prism-cell laser light-scattering spectrometer, which allowed us to perform DLS measurements of suspensions of isolated Limulus thick myofilaments in the relaxed state at a scattering angle as low as 3°. By considering the spectrum of the scaled average line width ($\bar{\Gamma}/K^2$) as a function of K^2, several interesting hydrodynamic phenomena of the thick myofilaments, as well as the conformation of myofilaments in suspension, were obtained. A comparison of the experimental results with the theoretical prediction based on the rigid-rod and the flexible-rod models is discussed.

II. Experimental Methods

A. Light Scattering. Two light-scattering spectrometers were used, one (LSSA) for making measurements at scattering angles between 25° and 120° and another (LSSB) for making measurements at small scattering angles down to ~3°.

LSSA has been described previously.[3,4] It used a cylindrical sample cell with an o.d. of 1 cm, an argon ion laser operated at $\lambda_0 = 514.5$ nm, and a Brookhaven BI2030 autocorrelator. LSSB used a thick piece of polished flat glass as the entrance window and a right-angle prism as the exit window for the (flow) sample cell. With this arrangement, DLS measurements could be conducted down to 2° without heterodyne beating of the scattered light with the stray light acting as the local oscillator for an aqueous suspension of polystyrene latex spheres.[11,12] The prism cell had two outlets connected to a circulating system, which was used for the purification of the filament suspension as shown in Figure 1. The argon ion laser was operated at $\lambda_0 = 488$ nm, and a Malvern Loglin Model 7027 64-channel single-clipped correlator was used. The details of LSSB have been described elsewhere.[11,12]

B. Preparation of Filament Suspensions. Thick filaments isolated from the levators of the telson of Limulus (*Tachypleus polyphemus*) were used. Animals were obtained from Marine Biological Laboratories, Woods Hole, MA, or were caught in Long Island Sound, Belle Terre, NY, or in the Great South Bay, NY. The molecular weight of thick myofilament of Limulus striated muscle was determined to be $(6.01 \pm 0.48) \times 10^8$ Da as measured by STEM using TMV as a standard. As the thick filaments were very strong scatterers, after isolation with the method described in ref 3, the filament suspension was already clean enough for making measurement at scattering angles larger than 15°. For measurements at smaller scattering angles, further removal of the dust particles was crucial. The thick filaments were first separated and purified with gradient centrifugation as described in ref 3. The dust particles in the solution were then removed by circulating the suspension through an agarose-bead (BIO-

* To whom all correspondence should be addressed.
† Department of Chemistry, State University of New York at Stony Brook.
‡ Present address: Department of Chemistry, University of Toronto, Toronto, Ontario M5S 1A1, Canada.
§ Department of Anatomical Sciences, State University of New York at Stony Brook. Present address: Department of Physiology and Biophysics, State University of New York at Stony Brook.
∥ Mitsubishi Kasei Institute of Life Sciences.
⊥ Department of Materials Science and Engineering, State University of New York at Stony Brook.

0024-9297/91/2224-0610$02.50/0

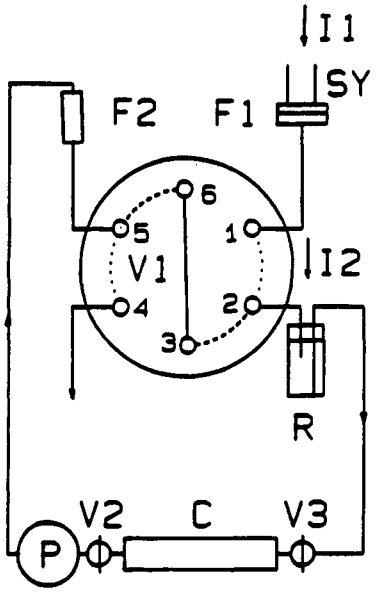

Figure 1. Closed filtration circuit used for the removal of dust particles from the myofilaments suspension: F1, Millipore filter holder; F2, column filled with agarose beads (BIO-RAD Bio Gel A-5m, 50–100 mesh); V1, 3-way Teflon valve (Rheodyne Inc., Model 50); V2 and V3, 2-way Teflon stopcocks; C, prism cell: P, pump (Fluid Metering Inc., Model RHOCTC); R, reservoir of ~1-mL capacity with septum cap. A filament suspension was introduced into the circulation system through the inlet I2; SY, syringe; I1, inlet for buffer solution. The dotted line shows connections in the valve V1 as the valve was set at position 1 (ports 1 and 2, 4 and 5, and 3 and 6 were connected). This was the position used during flushing of the system. The dashed line shows connections in the valve V1 as the valve was set at position 2 (ports 2 and 3, 5 and 6, and 3 and 6 were connected). This was the position used during purification of the filament suspension through the gel column F2.

RAD Bio Gel A-5m, 50–100-mesh) column. The sample cell formed a part of the filtration system (Figure 1). Buffer solution (100 mM KCl, 5 mM $MgCl_2$, 5 mM EGTA, 2 mM ATP, 5 mM Tris, pH 7.4) was first introduced by a syringe (Figure 1, SY) through a filter (Figure 1, F1, Millipore Millex-GV 0.22 μm) into the system. The whole circulatory system was flushed by the buffer solution with V1 at position 1. V1 was then turned to position 2, the filament sample was added through I2 and circulated in the closed circuit until the light beam in the sample cell looked homogeneous and no shining particles could be observed. The concentration of the filament in the suspension was also reduced appreciably by filtration through the agarose-bead column. However, it was still high enough for our DLS measurements. The sample concentration, as very roughly estimated by light-scattering intensity measurements at $\theta = 120°$, was $\lesssim 0.1$ μg/mL. All measurements were performed at 25 ± 1 °C.

III. Results

DLS measurements were performed with both LSSA and LSSB at large and small scattering angles, respectively. Figure 2 shows a linear plot of the K^2 scaled average characteristic line width ($\bar{\Gamma}/K^2$) versus K^2 from the cumulants fitting procedure.[13] The data used were obtained from four sets of experiments with the filaments from different animals. They could be fitted with a second-order cumulant for K^2 smaller than 4×10^9 cm^{-2} and with a fourth-order cumulant for the rest.

For a closer look at the K^2 dependence of $\bar{\Gamma}/K^2$, the data are plotted in a semilogarithmic scale (Figure 3) over a range of K^2 [8.5×10^7 cm$^{-2} < K^2 < 2.0 \times 10^9$ cm^{-2}], which corresponds to $3.7 < KL < 18$, if we take $L = 4.0$ μm. The values of $\bar{\Gamma}/K^2$ are relatively constant at $KL \lesssim 5$. Although we have not achieved $KL < 1$ for the muscle filament

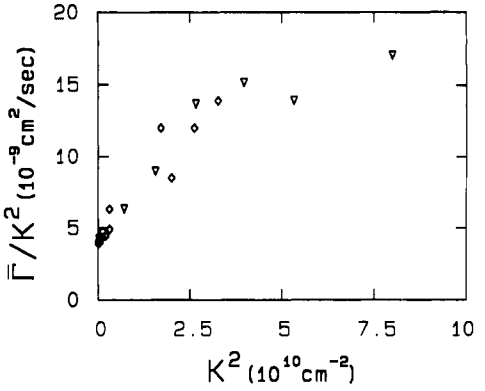

Figure 2. Linear plot of $\bar{\Gamma}/K^2$ vs K^2 of Limulus thick filament suspension over a wide range of scattering angles. Hollow diamonds were data obtained with LSSB and hollow triangles obtained with LSSA.

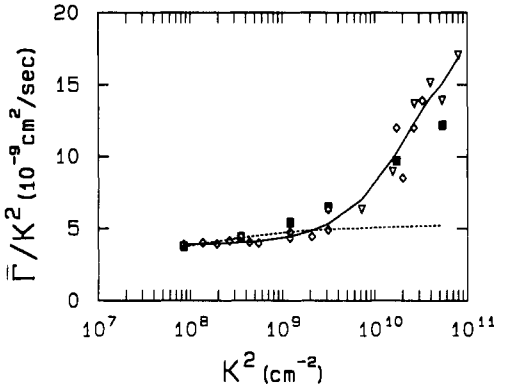

Figure 3. Semilogarithmic plot of $\bar{\Gamma}/K^2$ vs K^2. The data used were the same as that of the linear plot as shown in Figure 2. The solid line is a polynomial fitting of the data. The equation adopted is $\bar{\Gamma}/K^2 = 3.88 \times 10^{-9}(1 + 1.27 \times 10^{-10}K^2 - 1.97 \times 10^{-21}K^4 + 1.13 \times 10^{-32}K^6)$ cm^2/s. The filled squares are the theoretical prediction for flexible filaments in dilute solution with $L = 4.00$ μm, $d = 24$ nm, $D_T = 3.60 \times 10^{-9}$ cm^2/s, $D_1 = 2.97 \times 10^{-9}$ cm^2/s, $\Theta = 0.170$ s^{-1}, and $\gamma L = 0.10$. D_1 and Θ values were estimated from the D_T value with L and d by using Broersma's formula.[15,19] The dashed line is the theoretical simulation for a rigid isotropic thin rod with the same parameters as for a flexible filament but with $\gamma L = 0.0$.

suspensions, the relatively constant values of $\bar{\Gamma}/K^2$ over a range of KL ($3.5 < KL < 5$) suggested a lack of faster internal motion contributions to $\bar{\Gamma}/K^2$. The regularized Laplace inversion[14] of the time correlation function obtained over this K regime yielded a very narrow line-width distribution. Figure 4 shows a typical characteristic line-width distribution resolved from the intensity–intensity time correlation function by CONTIN at $\theta \sim 3°$. From the semilogarithmic plot, several important and unexpected features could be revealed. First, if we take the intercept of the linear extrapolation in $\bar{\Gamma}/K^2$ versus K^2 as the value for the overall translational diffusion coefficient ($\bar{\Gamma}/K^2|_{K^2 \to 0} = D_T$), the D_T ($=3.88 \times 10^{-9}$ cm^2/s) value is about 60% smaller than that of the calculated value according to the equation given by Newman et al.[15] for rigid rodlike particles by using the dimensions of the thick filaments obtained from electron microscopy (the length $L = 4.0$ μm and the diameter $d = 24$ nm[4]). $D_{T,Newman} = 6.47 \times 10^{-9}$ cm^2/s. Second, the $\bar{\Gamma}/K^2$ value is more than tripled at large scattering angles, which could not be predicted by any known rigid-body models. Most of the rigid-body models, such as a disk, a rod, or an ellipsoid, could only cause a maximum increase of the $\bar{\Gamma}/K^2$ value to about twice that of the base line $\bar{\Gamma}/K^2$ value due to translational motions because of the additional par-

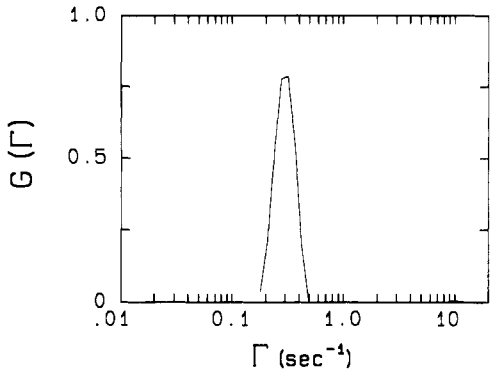

Figure 4. Line-width distribution from CONTIN[14] fitting of the intensity–intensity time autocorrelation function obtained at $K^2 = 8.5 \times 10^7$ cm^{-2} and 25 °C, $\lambda_0 = 488$ nm, variance $(\mu 2/\bar{\Gamma}^2) = 0.03$, and $\bar{\Gamma} = 0.312$/s ($\bar{D} = 3.69$ cm^2/s) with $\mu 2 = \int G(\Gamma)(\Gamma - \bar{\Gamma})^2 \, d\Gamma$ and $G(\Gamma)$ being the normalized line-width distribution. The narrow line-width distribution suggests an absence of internal motions in a relatively monodisperse suspension of myofilaments.

ticipation of only the rotational motion. Last, the internal motions of such a long structure at $KL = 3.7$ were not detected.

IV. Discussion

In a recent DLS and electron microscopy investigation of aqueous suspensions of synthetic myosin filaments in three different ionic strengths, Mochizuki-Oda and Fujime[8] have also observed the same phenomenon; i.e., the equation for D_T of a rigid rod would always yield a 60% larger value of D_T than that of the measured value ($\Gamma/K^2|_{K^2\to 0}$), if the length and the diameter from electron microscopy and sedimentation measurements in different ionic strengths were used. It is remarkable that we reached the same scaled results for D_T, although their species were 9 times shorter ($L \sim 470$ nm) than ours. The authors attributed the difference between the experimental value and the theoretical one to the anomalous friction between solvent molecules and the filament unit due to the myosin heads projecting from the shaft of the filament. The anomalous friction leads to either a 4 times larger apparent hydrodynamic diameter ("hydrodynamic envelope") in a projection model with normal viscosity or a 60% higher viscosity in a bare shaft model (e.g., see eq 2) with a normal hydrodynamic diameter. The two models are almost equivalent as far as the bending motion is concerned.

Furthermore, the muscle filaments are not rigid rods in suspension. Intuitively, one could imagine that such an inhomogeneous rod, with the ends and waist of the filament being thinner than the rest of the body[4] and the presence of internal cross-bridge motions, must be flexible. Both the flexibility of the filament and the internal cross-bridge motions must affect the intensity–intensity time correlation function.

Maeda and Fujime derived an expression for the spectrum of DLS of semiflexible (or bending) filaments in dilute and semidilute suspensions. In their model, the effects of anisotropic translational motions, the end-over-end rotational motion, the coupling between the translational motion and the rotational motion, and the flexibility or bending of the thick filaments have all been taken into account[10,16-18]

$$\bar{\Gamma}/K^2 = D_T + \frac{L^2}{12}\Theta f_1^*(KL) + (D_3 - D_1)\left[f_2^*(KL) - \frac{1}{3}\right] + \frac{k_B T}{\zeta L}\sum_m{}'' a_m(KL) + \Delta \quad (1)$$

where D_1, D_3, and Θ are the coefficients of sideways translation, lengthways translation, and end-over-end rotation, respectively; ζ is the friction constant per unit length of the filaments; $f_1^*(KL)$ ($f_1^*(0) = 0$ and $f_1^*(\infty) = 1$) and $f_2^*(KL)$ ($f_2^*(0) = {}^1/_3$ and $f_2^*(\infty) = 0$) are functions originating from the coupling of the motions and the anisotropy of the translational motion and depending only on KL; $a_m(KL)$ accounts for the effect on different bending (flexibility) modes (m) through a flexibility parameter γL (γ is the reciprocal of the statistical length); k_B is the Boltzmann constant and T is the absolute temperature. Δ is the contribution from cross-bridge motions. In eq 1, the first term is due to the overall translation D_T ($=[2D_1 + D_3]/3$), the second term to rotation, the third term to anisotropy in translation, and the fourth term to bending or flexibility of the filaments. The limiting values for eq 1 are $\bar{\Gamma}/K^2|_{K^2\to 0} = D_T$ and $\bar{\Gamma}/K^2|_{K^2\to\infty} = D_1 + (L^2/12)\Theta + (k_B T/\zeta L)m$ (without cross-bridge contributions).

For a *smooth* rigid rod with length L and diameter d, Broersma's formula gives the diffusion coefficients[15]

$$D_1 = \frac{k_B T}{4\pi\eta L}\left[\ln\left(\frac{2L}{d}\right) - 0.19 + 4.2\left\{1/\ln\left(\frac{2L}{d}\right) - 0.39\right\}^2\right] \quad (2a)$$

$$D_3 = \frac{k_B T}{2\pi\eta L}\left[\ln\left(\frac{2L}{d}\right) - 1.27 + 7.4\left\{1/\ln\left(\frac{2L}{d}\right) - 0.34\right\}^2\right] \quad (2b)$$

$$\Theta = \frac{3k_B T}{\pi\eta L^3}\left[\ln\left(\frac{2L}{d}\right) - 1.45 + 7.5\left\{1/\ln\left(\frac{2L}{d}\right) - 0.27\right\}^2\right] \quad (2c)$$

In eq 2, η is the solvent viscosity.

As there were few experimental DLS results of thick filaments in suspension, most of the comparisons of the theoretical predictions were done with simulated values or with experimental results for fd virus, which had a much smaller characteristic dimension. In the present study, we have simulated the $\bar{\Gamma}/K^2$ versus K^2 curves according to eqs 1 and 2. However, since the equation given by Newman et al. could not be used to predict L or d values correctly from the $D_T|_{K^2\to 0}$ value, we have used different L and γL values in the computation in order to get a best fit with our experimental result. The fact that Broersma's formula for smooth rigid rods were used for the analysis of DLS data even at $K^2 \to 0$ suggested only an effective diameter for the muscle filaments with cross bridges. The filled squares in Figure 3 show a best fit with $L = 4.0$ μm, which is very close to the direct observation from dark-field optical microscopy measurement using fluorescent labeled thick filaments,[4] and $\gamma L = 0.1$. As a comparison, a dashed line in Figure 3 shows the simulation with $L = 4.0$ μm and $\gamma L = 0.0$, i.e., a rigid rod. It is clear that, at small values of K^2, both rigid and flexible models basically yield the same result as the experimental result. But with increasing values of K^2, the $\bar{\Gamma}/K^2$ value from the rigid rod model remains flat and becomes much smaller than the measured one. According to eq 1 the rising of the $\bar{\Gamma}/K^2$ values is basically from different bending modes. It should be emphasized that the continuous elastic filament model that we have used to compare experimental data does not include contribution from cross-bridge motions[18] and the model is insufficient to account for the rapid rise in $\bar{\Gamma}/K^2$ at high K value. The model produces $\bar{\Gamma}/K^2$ values *slightly* above the experimental data in the intermediate scattering angle region ($K^2 = (3 - 7) \times 10^9$ cm^{-2}) but below the experimental data in the larger scattering angle region ($K^2 > 2 \times 10^{10}$ cm^{-2}). This observation could imply that the first (or second) bending

mode(s) in the real system was suppressed, causing a smaller rise in $\bar{\Gamma}/K^2$ in the intermediate scattering angle region; but additional internal motions have to be taken into account in order to account for the sharp rise of $\bar{\Gamma}/K^2$ values at large scattering angles. One of the possible sources for such motions is the cross-bridge motion. The intrinsic cross-bridge structure of the filaments would be different when compared with a homogeneous flexible rod. Extensive DLS studies[3,4] have shown that the cross-bridge motions are much more pronounced in the activated state than that in the relaxed state. Thus, incorporation of cross-bridge motions especially in the activated state should be a worthwhile undertaking. Electron microscopy measurements showed such muscle filament suspensions to be quite monodisperse. Consequently, there would be negligible fast dynamic motions due to the small filaments in the analysis of DLS data at high scattering angles. One might also argue that as eq 1 was still imperfect, even for smooth semiflexible chains, the deviation at large K^2 values could then be attributed to the weakness of the model, not to cross-bridge motions. This conclusion, however, cannot support the changes in cross-bridge motions for muscle filaments in the activated state.

In this paper, we presented the first DLS spectrum of thick myofilaments in aqueous suspension covering a wide scattering angular range including measurements at very small scattering angles with $\theta \sim 3°$. The ability to measure DLS in the self-beating mode at such small scattering angles represents one essential accomplishment of this experiment since the thick filaments are 4 μm in length. Thus, measurements of pure translational diffusive motions require our ability to perform the small-angle DLS measurement. Furthermore, at very small scattering angles, clarification of the muscle filament suspension became another obstacle that we had to overcome. A comparison of $\bar{\Gamma}/K^2$ versus K^2 data with the continuous elastic filament models clearly showed that such models without introduction of cross-bridge motions were inadequate. The result demonstrated the limitations of DLS methodology for very large filaments with complex structures and showed several interesting features that would require difficult theoretical development of filament dynamics including cross-bridge motions for a better understanding of the mechanism of muscle contraction as viewed by DLS.

Acknowledgment. We gratefully acknowledge support of this project by the National Science Foundation, Polymers Program (DMR 8921968).

References and Notes

(1) Huxley, H. E. *Science* **1967**, *164*, 1356.
(2) Huxley, A. F. *J. Physiol.* **1974**, *243*, 1.
(3) Fan, S.-F.; Dewey, M. M.; Colflesh, D. E.; Gaylinn, B.; Greguski, R. A.; Chu, B. *Biophys. J.* **1985**, *47*, 809.
(4) Kubota, K.; Chu, B.; Fan, S.-F.; Dewey, M. M.; Brink, P.; Colflesh, D. E. *J. Mol. Biol.* **1983**, *166*, 329.
(5) Fan, S. F.; Dewey, M. M.; Colflesh, D.; Chu, B. *Biophys. J.* **1987**, *52*, 859.
(6) Newman, J.; Carlson, F. D. *Biophys. J.* **1980**, *29*, 37.
(7) Haskell, R. C.; Carlson, F. D. *Biophys. J.* **1981**, *33*, 39.
(8) Mochizuki-Oda, N.; Fujime, S. *Biopolymers* **1988**, *27*, 1389.
(9) Suzuk, N.; Wada, A. *Biochim. Biophys. Acta* **1981**, *670*, 408.
(10) Maeda, T.; Fujime, S. *Macromolecules* **1981**, *14*, 809.
(11) Chu, B.; Xu, R. In *OSA Proceedings on Photon Correlation Techniques and Applications*; Abbiss, J. B., Smart, A. E., Eds.; 1989; Vol. 1, pp 137–146.
(12) Chu, B.; Xu, R.; Maeda, T.; Dhadwal, H. S. *Rev. Sci. Instrum.* **1988**, *59*, 716.
(13) Koppel, D. J. *Chem. Phys.* **1972**, *57*, 4814.
(14) Provencher, S. *Comput. Phys. Commun.* **1982**, *27*, 213, 229.
(15) Newman, J.; Swinney, H. L.; Day, L. A. *J. Mol. Biol.* **1977**, *116*, 593.
(16) Maeda, T.; Fujime, S. *Macromolecules* **1984**, *17*, 1157.
(17) Maeda, T.; Fujime, S. *Macromolecules* **1984**, *17*, 2381.
(18) Fujime, S.; Kubota, K. *Macromolecules* **1984**, *17*, 441.
(19) Broersma, S. J. *Chem. Phys.* **1960**, *32*, 1626, 1632.